DOI: 10.1002/ (())
Article type: Communication

Novel Dopant-Free D-π-D-π-D Conjugated Hole Transport Materials with Tunable Energy Levels for Efficient and Stable Perovskite Solar Cells

Fei Zhang[+], *Xicheng Liu*[+], *Chenyi Yi, Dongqin Bi, Jingshan Luo, Shirong Wang*[*], *Xianggao Li*[*], *Yin Xiao , Shaik Mohammed Zakeeruddin*[*], *Michael Grätzel*[*]

[a]F.Zhang, Prof.S.Wang*, Prof. X.Li*, Dr. Y.Xiao
School of Chemical Engineering and Technology, Tianjin University
300072 Tianjin, China
Email: wangshirong@tju.edu.cn;lixianggao@tju.edu.cn

[b]F.Zhang, Dr.C.Yi, Dr.D.Bi,Dr.J.Luo, Dr.S.M.Zakeeruddin*, Prof.M.Grätzel *
Laboratory of Photonics and Interfaces, Institute of Chemical Sciences and Engineering,
École Polytechnique Fédérale de Lausanne (EPFL)
Station 6 CH-1015, Lausanne, Switzerland
Email: shaik.zakeer@epfl.ch ; michael.graetzel@epfl.ch

[c]F.Zhang, Prof.S.Wang*, Prof. X. Li*, Dr.Y.Xiao
Collaborative Innovation Center of Chemical Science and Engineering (Tianjin)
300072 Tianjin, China

[d]X.Liu,
School of Chemistry and Chemical Engineering, Qufu Normal University,
273165 Qufu, China

+ F.Zhang and X.Liu have the equivalent contribution

Keywords: hole transport material; dopant-free; perovskite solar cell; low-cost

Abstract: Three novel hole transporting materials (HTM) using the 4-Methoxytriphenylamine (MeOTPA) core were designed and synthesized.The HTMs energy levels were tuned to match with perovskite by introducing electron donating groups symmetrically linked with olefinic bonds as the π bridge. The $CH_3NH_3PbI_3$-based perovskite solar cells exhibited a remarkable overall power conversion efficiency (PCE) of 16.1 % without any dopants and additives based on 4-((*E*)-4-(bis(4-methoxyphenyl)amino)styryl)-*N*-(4-((*E*)-4-(bis(4methoxyphenyl)amino) styryl)phenyl)-*N*-(4-methoxyphenyl)aniline (Z34) , which is comparable to 16.7 % obtained by p-doped *spiro*-OMeTAD-based device. Importantly, the devices based-on three HTMs show relatively better stability compared to devices based on *spiro*-OMeTAD when aged under ambient air of 30% relative humidity in the dark.

Increasing energy demands and concerns about global warming drive the exploration of clean, inexpensive and renewable energy sources. Recently, the photovoltaic community has witnessed a rapid emergence of a new class of solid-state heterojunction solar cells based on solution-processable organometal halide perovskite absorbers [1-3]. The power conversion efficiency (PCE) of solid-state perovskite solar cells (PSCs) has been quickly increased to over 20% [4-6] because of their unique characteristics, such as a broad spectral absorption range, large absorption coefficient, high charge carrier mobility and long diffusion length. [2]

In the configuration of a PSC, the hole transporting material (HTMs) plays the key role of promoting hole migration, as well as preventing internal charge recombination. [7] A great number of HTMs have been developed and applied in PSCs, including various newly designed, inorganic p-type semiconductors, conducting polymers, as well as small molecule hole conductors [8]. 2,2′,7,7′-tetrakis(*N*,*N*-di-*p*-methoxyphenylamine)-9,9′-spirobifluorene (*spiro*-OMeTAD) that was well studied in solid state DSCs, continues to exhibit high performance in PSCs. Due to its relatively low hole mobility and its tedious synthesis strongly correlated to its production cost, numerous alternative HTMs have been explored with an aim to replace such a material [9-20]. Although inorganic HTMs (CuI and CuSCN) have drawn much attention due to their high hole mobilities and low production cost [21],polymeric HTMs, such as conjugated polytriarylamine (PTAA) [22], poly(3-hexylthiophene-2,5-diyl) (P3HT) [23] *etc*., have also shown competitive performances in PSCs, small molecular HTMs have advantages of their convenient purification, controllable molecular structures and relatively high efficiency [24].Regarding small molecule HTMs incorporated with dopants, the PCE of the dopant-free HTM based devices are consistently lying between 10% to 13% [25-36], few are over 15%.[37-40]

Herein, we report the synthesis and characterization of three novel dopant-free 4-Methoxytriphenylamine (MeOTPA) -based HTMs as shown in **Figure** 1a, as well as their application in perovskite solar cells. The energy levels of the HTMs can be tuned by attaching

to the MeOTPA core with different electron donating groups by olefinic bonds. The device, fabricated with Z34 as HTM, achieves a PCE of 16.1 %without doping under AM 1.5G (100 mW cm^{-2}) illumination. This result is comparable to that obtained using the well-known p-type doping *spiro*-OMeTAD (16.7 %). Moreover, the three HTMs based devices presented a better stability than that based on *spiro*-OMeTAD under ambient air condition of 30% relative humidity without encapsulation after 1000 h in the dark. The cost of the new HTMs is around 1/10 of that of *spiro*-OMeTAD.

The MeOTPA -core HTMs were synthesized by Wittig reaction with cheap starting materials. The synthetic route for the HTMs is depicted in **Figure 1b** and experimental details are given in the Experimental Section.† The new MeOTPA derivatives (Z33,Z34 and Z35) were fully characterized by ^{1}H NMR spectroscopy, high resolution mass spectrum, and elemental analysis. All the analytical data are consistent with the proposed structures. All of them show good solubility in common organic solvents, such as dichloromethane, chloroform, tetrahydrofuran and toluene, etc. We also roughly estimated the synthesis cost of 1 gram Z33, Z34 and Z35 and the details are shown in the supporting information. The estimated synthesis cost of Z33, Z34 and Z35 is 70 $/g, 66 $/g and 54 $/g, respectively which is much cheaper than that of *spiro*-OMeTAD (598 $/g).

The UV-Vis absorption spectra of Z33, Z34 and Z35 in THF solution and on thin film state are shown in **Figure 2a**, and the corresponding data are summarized in Table 1. As shown in **Figure 2a**, all of them show two absorption bands at 300-320 nm and 400-450 nm regions. The absorption bands in 300-320 nm region can be assigned to the n-π* transition of the TPA moieties. The absorption in 400-450 nm is attributed to the intramolecular charge transfer (ICT) of π-π* transition. [41] Due to the smaller conjugated degree, [42] the ICT peak ($\lambda_{abs/max}$) of Z35 shows a blue shift compared with Z33 and Z34.

Thermogravimetric analysis (TGA) and differential scanning calorimetry (DSC) measurements show that these three HTMs have high decomposition temperatures (T_d, 432.3

ºC,417.2 ºC and 402.5 ºC for Z33, Z34 and Z35, respectively) and glass transition temperatures (T_g, 96.2 ºC,106.1 ºC and 89.1 ºC for Z33,Z34 and Z35, respectively) (**Figure S1a**, ESI†).

To understand the charge-carrier transport properties of these HTMs, their hole mobilities (μ) were determined from transit times (t_T, ESI **Figure S3**) with equation of $\mu = d^2 / Vt_T$.[43] Here d is the organic film thickness, V applied voltage. At room temperature, hole mobilities of Z33, Z34 and Z35 are 4.67×10^{-4} cm^2 V^{-1} s^{-1},7.46×10^{-4} cm^2 V^{-1} s^{-1} and 2.76×10^{-4} cm^2 V^{-1} s^{-1} at the electric field of 1.0×10^5 V cm^{-1}, respectively, all of them are higher than that of pristine *spiro*-OMeTAD (2×10^{-4} cm^2 V^{-1} s^{-1} at the electric field of 2.6×10^5 V cm^{-1}).[44]

Density functional theory (DFT) calculations were carried out in order to understand the electronic structure and the energy levels of the HTMs. The optimized molecular geometries, the highest occupied molecular orbital (HOMO) levels and the lowest unoccupied molecular orbital (LUMO) energy levels were shown in **Figure S2.** The LUMO distribute mainly on the part of the peripheral units close to the triphenylamine core while the HOMO energy levels distribute mainly on the central triphenylamine core and the extended vinyl bridge. The calculated HOMO levels of three HTMs are estimated to be -4.35 eV,-4.23 eV and -4.38 eV for Z33, Z34 and Z35, respectively.

Furthermore, their energy levels are experimentally determined by photoemission yield spectroscopy (PYS). According to PYS result (**Figure S1b**,ESI), the HOMO energy level of Z33 is -5.34 eV while that of Z35 is -5.42 eV , slightly lower than that of *spiro*-OMeTAD (-5.22 eV) [45], whereas the HOMO energy level of Z34 is -5.14 eV ,higher than that of *spiro*-OMeTAD, as shown in **Figure 2b**. Moreover, the optical band gap (E_g) is calculated from the absorption onset wavelength (E_g=1240/λonset) of the corresponding absorption spectrum, indicating that the E_g is 2.72, 2.71 and 2.81 eV for Z33, Z34 and Z35 respectively. The LUMO levels of HTMs are calculated to be -2.62 eV,-2.43 eV and -2.61 eV, which are more positive than that of $CH_3NH_3PbI_3$ (-3.91 eV).[46] These results agreed well with the trend

derived from DFT calculations. Thus, these three HTMs can not only act as a hole transporting layer, but also play as an electron blocking layer in the PSCs.

The steady-state PL spectra are shown in **Figure 2c**. Strong PL quenching was observed when the HTM materials were coated on perovskite films. For the three HTMs coated perovskite films, the PL intensity was reduced to roughly 26%, 20% and 46% of that from pristine films for Z33, Z34 and Z35 respectively, suggesting that Z34 can extract charge carrier more efficiently than the other two HTMs. The hole extraction capacities of Z33-Z35 at glass/$CH_3NH_3PbI_3$/HTMs interfaces have been investigated by time-resolved photoluminescence (TRPL) measurement. **Figure 2d** presents the measured PL decay spectra and the corresponding decay time are obtained by fitting the data with biexponential decay function.[47] The PL decay lifetime is reduced to 82.8 ns, 63.1 ns and 107.9 ns for devices with Z33, Z34 and Z35 in comparison with 121.8 ns for the device without HTM layer. From these observations, we conclude that hole injection from the valence band of perovskite into the HOMO of Z34 is more efficient than the other two HTMs.

The schematic diagram of the perovskite solar cells applied in this study are shown in **Figure 3a**. The perovskite solar cells were fabricated by sequential deposition using a similar method as reported in our recent paper.[48] **Figure 3b** presents a cross-sectional scanning electron microscopy (SEM) image of the perovskite solar cell indicating clearly the infiltration of $CH_3NH_3PbI_3$ perovskite into the TiO_2 pores forming a perovskite/TiO_2 nanocomposite which is covered by a perovskite capping layer. We evaluated the photovoltaic performance of perovskite solar cells based on the three HTMs and *spiro*-OMeTAD with or without doping. The photocurrent densitiy-voltage (*J–V*) curves under AM 1.5G irradiation of 100 mW cm^{-2} are presented in **Figure 3c** and **Figure S4a** and the photovoltaic parameters are summarized in Table 2. The average PCE of the devices based on three HTMs varies from 10.8% for Z35 to 15.9% for Z34. The lower performance shown by Z35 is mainly related to an insufficient driving force for hole injections related to its deeper HOMO energy level (–

5.42 eV) as compared to the valence band of $MAPbI_3$ (–5.43 eV). As expected, Z33 gives a higher V_{oc} (1.087 V) than *spiro*-OMeTAD (1.078 V) for the device, which is commensurate with its lower HOMO level, while Z34 gives a lower V_{oc} (1.055 V) than *spiro*-OMeTAD due to its higher HOMO level.The best device based on Z34 affords an open-circuit voltage (V_{oc}) of 1.055 V, a short-circuit current density (J_{sc}) of 21.2 mA cm^{-2} and a fill factor (FF) of 0.70, leading to a PCE of 16.1 % under AM 1.5G (100 mW cm^{-2}) illumination. This result is comparable to that of *spiro*-OMeTAD (16.7 %) doped with lithium bis(trifluoromethylsulfonyl)imide (LiTFSI) and *4-tert*-butylpyridine (tBP). However, devices based on doped three HTMs exhibit lower photovoltaic performance compared to dopant-free HTMs, especially in terms of FF and J_{sc}. It is partly because of that the dopants that work well with spiro-OMeTAD might not be suitable for these three HTMs. [49] Moreover, the dopants seem to have a negative impact on film morphology whcih can be seen from the SEM image in **Figure S5**. Similar behavior was observed with other reports.[40,50] In the absence of dopants, *spiro*-MeOTAD based devices generated a PCE of only 3.92% due to the significant lowering of V_{oc} and *FF* compared to the doped devices. Hysteresis behavior is frequently observed in perovskite solar cells. A small hysteresis was observed in the *J–V* curves, the measured PCEs differences are 1%, 3%, 10% and 1% for Z33, Z34, Z35 and *spiro*-OMeTAD, respectively. The stabilized power outputs from devices based on *spiro*-OMeTAD and Z33-Z35 are 16.6%, 15.2%, 16.1% and 11.2% respectively **(Figure S6)**, consistent with the obtained PCE.

The J_{sc} of the PSC devices shows linear relationship with light intensities **(Figure S**4 b), indicating that the charge collection ability of HTM containing devices are independent of light density. According to previous investigations, it can be inferred that no space charge limited photocurrent occurs in the devices with Z33-Z35 because of faster electrons and higher hole mobility .[51-53]

The incident photon-to-electron conversion efficiency (IPCE) spectrum of the cell with the four HTMs is presented in **Figure 3d**. The integrated current densities estimated from the IPCE spectra (20.30 mA cm^{-2}, 20.90 mA cm^{-2}, 17.96 mA cm^{-2} and 20.80 mA cm^{-2} for Z33, Z34, Z35 and *spiro*-OMeTAD, respectively) are in good agreement with the J_{sc} values obtained from the *J-V* curves. We fabricated batches of 10 cells each using the three HTMs and *spiro*-OMeTAD and demonstrate in **Figure 4** excellent reproducibility by the narrow statistical distribution of the photovoltaic metrics**.**

We compared the stability of Z33-Z35 and *spiro*-OMeTAD -based perovskite solar cells by exposing them to ambient air of 30% relative humidity without encapsulation and showed in **Figure 5** the time evolution of the photovoltaic metrics. The devices based-on Z33 and Z34 show a slight increase of the PCE, while that based-on *spiro*-OMeTAD and Z35 decrease after 1000 h at room temperature in ambient air of 30% relative humidity without encapsulation. The devices based-on Z33 and Z34 obtained a slight increase of the PCE, that might be due to the better conductivity of the HTM after oxygen doping during the aging test which can be seen from the **Figure S6**. The three HTMs based devices exhibited better stability which was mainly attributed to their lack of deliquescent doping additives[54,55].

In summary, we synthesized three novel D-π-D-π-D conjugated HTMs (Z33, Z34 and Z35) with simple low cost process. The HOMO and LUMO energy levels of these MeOTPA derivatives are effectively tuned to match with perovskite by introducing electron-donating groups symmetrically linked with olefinic bonds as the π bridge, which is demonstrated by optical and electrochemical studies. The perovskite solar cell based on Z34 as HTM without doping affords an impressive PCE of 16.1%, which is comparable to that obtained employing the well-known p-doping *spiro*-OMeTAD. The devices based on Z33-Z35 obtained a higher stability than that of *spiro*-OMeTAD at room temperature aged in ambient air of 30% relative humidity without encapsulation after 1000 h under dark.Moreover, the cost of these HTMs is around 1/10 of that of *spiro*-OMeTAD. The introduction of these

three novel HTMs with easier synthesis, low cost and excellent performance highlight their potential use in the future deployment of perovskite solar cells.

4. Experimental Section

*Materials:*Materials were all available commercially and used without further purification if not mentioned specially. Compound (2), (3) and (4) were synthesized according to our previous literature. [56]

Materials measurements:^{1}H NMR spectras was recorded with an INOVA 400MHz spectrometer (Varian, USA). Mass spectra (MS) was performed on an Autoflex tof/tofIII mass spectrometer (Bruker, Germany). UV spectra of the HTMs in tetrahydrofuran (THF) solutions (1×10^{-5} mol L^{-1}) was recorded with Thermo Evolution 300 UV-Vis spectrometer (Thermo Electron, USA) in the 200-800 nm wavelength range at room temperature. Thermo gravimetrical analyses (TGA) were recorded with TA Q500 thermo gravimetric apparatus (TA Instruments, USA) at a heating rate of 10 °C min^{-1} under nitrogen atmosphere. Differential scanning calorimetry (DSC) was conducted on TA Q20 Instrument (TA Instruments, USA) at a heating rate of 10 °C min^{-1} under nitrogen atmosphere. Photoemission yield spectroscopy (PYS) instrument was PYS-202 ionization energy test system (Sumitomo Heavy Industries, Japan) at the voltage of 100 V, waiting time of 1 s and energy range from 4.0 to 8.5 eV. The time-of-flight (TOF) measurements were performed on TOF401 (Sumitomo Heavy Industries. Ltd. Japan), for which the samples were prepared through spin coating using a structure ITO/HTM (about 1μm)/Al (150nm) with an active area of 3×10 mm^2. The film thickness was performed on a surface profiler (P-6, KLA-Tencor, USA).

Synthesis of HTMs

4-((E)-4-(di-p-tolylamino)styryl)-N-(4-((E)-4-(di-p-tolylamino)styryl)phenyl)-N-(4-methoxyphenyl)aniline (Z33)

Compound **1** (0.17 g, 0.5 mmol) and **2** (1.26 g, 2 mmol) were added into a 100mL round-bottom flask under N_2.Anhydrous THF (40 mL) was added to above flask, cooled down to

0 °C. The THF solution of t-BuOK (16 mmol,0.8 mol L^{-1}) was added dropwise to above flask, stirred for 30 min at 0 °C, followed by stirring at room temperature until compound **1** was consumed completely (monitored by thin-layer chromatography). The reaction was terminated with ice water. The crude product was refluxed for 8 h in THF with a catalytic amount of iodine. Then the remaining iodine was removed by sodium hydroxide (NaOH) solution (Wt = 10%, 100 mL) with stirring for 2 h. After that, the product was purified by chromatographed on a silica gel column (petroleum ether: ethyl acetate =15:1 as eluent) to give the title compound as a pure compound Z33 (0.33 g, 77%): ^{1}H NMR (400 MHz, $CDCl_3$) δ 7.32 (t, *J* = 8.1 Hz, 8H), 7.15 – 6.81 (m, 32H), 3.80 (s, 3H), 2.31 (s, 12H). HRMS (m/z): 870.4403 [M+H], Calcd, 869.4345.Elemental Analysis: Found: C, 86.83; H, 6.36. Calc. for $C_{63}H_{55}N_3O$: C, 86.96; H, 6.37.

4-((E)-4-(bis(4-methoxyphenyl)amino)styryl)-N-(4-((E)-4-(bis(4 methoxyphenyl)amino)styryl) phenyl)-N-(4-methoxyphenyl)aniline (Z34)

Z34 was prepared and purified according to the procedure described for Z33, starting from compound **3** (1.32 g, 2 mmol) and **1** (0.17 g, 0.5 mmol).(0.32g, 68%): ^{1}H NMR (400 MHz, $CDCl_3$) δ 7.84 (d, *J* = 8.8 Hz, 1H), 7.68 (dd, *J* = 12.0, 7.3 Hz, 1H), 7.54 (d, *J* = 6.2 Hz, 1H), 7.50-7.43 (m, 1H), 7.31 (dd, *J* = 14.2, 8.6 Hz, 6H), 7.16-6.76 (m, 30H), 3.80 (d, *J* = 5.2 Hz, 15H). HRMS(m/z): 934.4224 [M+H], Calcd for $C_{63}H_{55}N_3O_5$: 933.4142. Elemental Analysis: Found: C, 81.15; H, 5.94. Calc. for $C_{63}H_{55}N_3O$: C, 81.00; H, 5.93.

4-((E)-2-(9-ethyl-9H-carbazol-3-yl)vinyl)-N-(4-((E)-2-(9-ethyl-9H-carbazol-3-yl)vinyl)phenyl-N-(4-methoxyphenyl)aniline (Z35)

Z35 was prepared and purified according to the procedure described for Z33, starting from compound **4** (1.10 g, 2 mmol) and **1** (0.17 g, 0.5 mmol).(0.25g, 70%): ^{1}H NMR (400 MHz, $CDCl_3$) δ (ppm): 8.20 (s, 2H), 8.11 (d, *J* = 7.7 Hz, 2H), 7.64 (d, *J* = 8.4 Hz, 2H), 7.48 - 7.32 (m, 10H), 7.26 - 7.03 (m, 14H), 4.33 (dd, *J* = 14.2, 7.0 Hz, 4H), 2.34 (s, 3H), 1.42 (t, *J* = 7.2

Hz, 6H). HRMS (*m/z)*: Found 714.3481 [M+H], Calcd , 713.3406. Elemental Analysis: Found: C, 85.82; H, 6.08. Calc. for $C_{51}H_{43}N_3O$: C, 85.80; H, 6.07.

*Solar cell fabrication:*Devices were prepared on conductive fluorine-doped tin oxide (FTO) coated glass substrates. The substrates were cleaned extensively by deionized water, acetone and isopropanol. A compact titanium dioxide (TiO_2) layer was deposited by spray pyrolysis of 4.5 ml ethanol solution containing 0.3 mL titanium diisopropoxide bis(acetylacetonate) solution and 0.2 mL acetylacetone at 450 ℃ in air. On top of this layer, a 200-300 nm-thick mesoporous titanium dioxide was formed by spin-coating 30 nm sized nanoparticles (30NRT, Dyesol) diluted in ethanol (1:6 *w*/*w*) at 5000 r.p.m. for 20 s. The formed layer was heated to 500 degrees and sintered for 0.5 h in oxygen atmosphere. The $CH_3NH_3PbI_3$ film was fabricated by sequential deposition using a similar method as developed by our recent paper. [48] The lead iodide (PbI_2, 1.2 M in a mixture of DMSO/*N,N*-dimethylformamide 1:4 v/v) was spin coated on the top of mesoporous TiO_2 layer at 4000 r.p.m. for 10 s and left for drying for 10 min at 70 ℃. Subsequently, on the top of a lead salt 0.1 M CH_3NH_3I isopropanol solution was sprayed and left for 90 s before spin coating at 3000 r.p.m. for 10 s followed by drying at 100 ℃ for 1 h. Subsequently, for devices with hole transporting materials *spiro*-MeOTAD and Z33-Z35 compounds were dissolved in chlorobenzene at the concentrations of 72.3 mg/mL (28.8 µl 4-tert-butylpyridine,17.5 µl of 520 mg ml^{-1} lithium bis(trifluoromethylsulphonyl)imide acetonitrile solution dissolved in 1 ml chlorobenzene) and 20 mg/mL respectively and deposited on the top of perovskite by spin coating at 4000 r.p.m. for 20 s. Devices were finalized by thermal evaporation of 80 nm thick gold layer.

*Device measurement:*For current-density-voltage (*J-V*) characteristics, the cells were illuminated under 100 mW cm^{-2} (AM 1.5G) by a 450 W Xenon lamp (Oriel), as a light source, equipped with a Schott K113 Tempax sunlight filter (Praezisions Glas & Optik GmbH) to match the emission spectra to the AM1.5G standard in the region of 350-750 nm., and the *J-V*

characteristics of the cells were recorded on Keithley (Model 2400) digital source meter. A mask with a window of 0.16 cm^2 was clipped to define the active area of the cell. The incident photon-to-electron conversion efficiency (IPCE) spectrum was obtained on measured by focusing light from the 300W Xenon lamp (ILC Technology, U.S.A.) through a Gemini-180 double monochromator (Jobin Yvon Ltd., U.K.) while chopping at 3 Hz before illuminating onto the photovoltaic cell.

Supporting Information

Supporting Information is available from the Wiley Online Library or from the author.

Author contributions:

F.Z. and C.Y.Y designed the experiment, F.Z carried out the experimental study on device fabrication and basic characterization. X.C.L and Y.X designed and synthesized the three hole-transporting material, also performed all the physical property tests and quantum chemical calculation. F.Z. and X.C.L calculated the cost of the three HTMs. D.Q.B. performed the IPCE and stability test. J.S.L. performed SEM measurements. Z.F. wrote the first draft of the paper. All the authors contributed to the discussion and the writing of the paper, and approved. S.M.Z. and X.G.L coordinated the research, whereas S.R.W. and M.G. supervised the project.

Acknowledgements

We thank Dr.Gwénolé Jacopin (Laboratory of Quantum Optoelectronics,EPFL) for the PL test and Dr. Xiong Li (LPI, EPFL) for fruitful discussions.This work was supported by the Key Projects in Natural Science Foundation of Tianjin (16JCZDJC37100).FZ thanks the China Scholarship Council for funding. MG. thanks the King Abdulaziz City for Science and Technology (KACST) for financial support. Financial support from the Swiss National Science Foundation (SNSF), the NRP 70 "Energy Turnaround", CCEM-CH in the 9th call proposal 906: CONNECT PV, the European Union’s Horizon 2020 research and innovation

programme under the grant agreement No 687008 (GOTSolar) as well as from SNF-NanoTera and Swiss Federal Office of Energy (SYNERGY) is gratefully acknowledged. The information and views set out in this article are those of the author(s) and do not necessarily reflect the official opinion of the European Union. Neither the European Union institutions and bodies nor any person acting on their behalf may be held responsible for the use which may be made of the information contained herein.

Received: ((will be filled in by the editorial staff))
Revised: ((will be filled in by the editorial staff))
Published online: ((will be filled in by the editorial staff))

[1]A.Kojima, K.Teshim, Y.Shirai ,T.Miyasaka, *J.Am.Chem.Soc*.**2009**, 131, 6050−6051.

[2]F.Zhang, S.R.Wang, X.G.Li, Y.Xiao, *Curr. Nanosci*. **2016**,12,137−156.

[3]F.Zhang, S.R.Wang, X.G.Li, Y.Xiao, *Synthetic Metals,***2016**,220,187-193.

[4]W.S.Yang, J.H.Noh, N.J.Jeon, Y.C.Kim, S.Ryu, J.Seo,S.I.Seok, *Science*, **2015**,348, 1234−1237.

[5]D.Q.Bi, W.Tress, M.I.Dar, P.Gao, J.S.Luo, C.Renevier, K.Schenk,A.Abate, F.Giordano, J.C.Baena, J.Decoppet, S.M.Zakeeruddin, M.K.Nazeeruddin, M.Grätzel, A.Hagfeldt, *Sci. Adv.* **2016**,2,e1501170.

[6]M.Saliba, S.Orlandi, T.Matsui, S.Aghazada, M.Cavazzini, J.Correa-Baena, P.Gao, R. Scopelliti, E.Mosconi, K.Dahmen, F.D.Angelis, A.Abate, A.Hagfeldt, G.Pozzi, M.Graetzel, M.K.Nazeeruddin, *Nat Energy*, **2016**,15017.

[7]T. Swetha, S.P.Singh, *J. Mater. Chem. A*, **2015**,**3**, 18329-18344.

[8]Z.Yu,L.C.Sun, *Adv.EnergyMater*,**2015**,5,1500213.

[9]J.H.Heo, S.H.Kim, J.H.Noh, T.N.Mandal, C.-S.Lim, J.A.Chang, Y.H.Lee, H.Kim, A. Sarkar, M.K.Nazeeruddin, M.Grätzel, S.I.Seok, *Nat. Photon.***2013***,*7, 486 -489.

[10]B.Xu, E.Sheibani, P.Liu, J.Zhang, H.Tian, N.Vlachopoulos, G.Boschloo, L.Kloo, A.Hagfeldt,L.Sun,*Adv.Mater,* **2014***,*26,6629-6634. .

[11]L.Zheng, Y.H.Chung, Y.Ma, L.Zhang, L.Xiao, Z.Chen, S.Wang,B.Qu, Q. Gong, *Chem.Commun.,***2014***,*50,11196-11199. .

[12]J.A.Christians, R.C.M.Fung, P.V.Kamat, *J.Am.Chem.Soc.***2014**,36,758-764. .

[13]A.Krishna , D.Sabba , H.Li, J. Yin , P. P. Boix , C. Soci ,S. G. Mhaisalkar , A. C. Grimsdale, *Chem.Sci.,***2014***,*5,2702-2709.

[14]J.J.Guo, X.F.Meng, J.Niu, Y.Yin, M.M.Han, X.H. Ma, G.S.Song, F.Zhang, *Synthetic Metals*, **2016**, 220,462-468.

[15]P.Qin, N.Tetreault, M.I.Dar, P.Gao, K.L.McCall, S.R.Rutter, S.D.Ogier, N.D.Forrest, J.S.Bissett, M.J.Simms, A.J.Page, R.Fisher, M.Grätzel, M.K.Nazeeruddin, *Adv.Energy. Mater.***2015***,*5,1400980.

[16]J.W.Jung, C.-C.Chueh,A.K.Y.Jen, *Adv.EnergyMater.,***2015**,5,1500486. .

[17] G. A. Sepalage , S. Meyer , A. Pascoe , A. D. Scully , F. Huang , U. Bach ,Y.B. Cheng , L.Spiccia, *Adv.Funct.Mater.,***2015***,*25,5650-5661.

[18]H. Li, K.Fu, A.Hagfeldt, M.Grätzel, S.G.Mhaisalkar, A.C.Grimsdale, *Angew. Chem.Int.*

*Ed.,***2014**,53,4085-4088..

[19]H.Kim, K.G.Lim, T.W.Lee, *EnergyEnviron.Sci.***2016**,9,12-30.

[20] K.G.Lim , H.B. Kim , J. Jeong , H. Kim , J. Y. Kim , T.W. Lee , *Adv.Mater.***2014***,* 26, 6461.

[21] P.Qin , S. Tanaka , S. Ito , N. Tetreault , K. Manabe , H. Nishino ,M. K. Nazeeruddin , M. Grätzel , *Nat. Commun.*,**2014**,5,3834.

[22] N. J. Jeon, J. H. Noh , W. S. Yang , Y. C. Kim , S. Ryu , J. Seo , S. I. Seok , *Nature,***2015***,* 517, 476 .

[23] M. Cai, V. T. Tiong , T. Hreid , J. Bell , H. Wang , *J. Mater. Chem. A*, **2015**,3, 2784-2793.

[24] J.Y. Xiao, L. Y. Han, L. F. Zhu, S. T. Lv, J. J. Shi, H.Y. Wei, Y. Z. Xu, J. Dong, X. Xu, Y. Xiao, D. M. Li, S. R. Wang, Y. H. Luo, X. G. Li, Q. B. Meng. *RSC Adv*, **2014**,4,32918-32923.

[25]S.T. Lv, Y.K. Song, J.Y. Xiao, L.F. Zhu,J.J. Shi, H.Y.Wei,Y.Z.Xu, J.Dong, X.Xua, S.R.Wang, Y. Xiao, Y.H.Luo, D.M.Li, X.G.Li, Q.B.Meng, *Electrochimica Acta*, **2015**, 182,733−741.

[26] M.Franckevicius, A.Mishra, F.Kreuzer, J.S.Luo, S.M.Zakeeruddin, M.Gratzel, *Mater. Horiz*,**2015**,2 , 613−618.

[27] S.Kazim, F. J. Ramos, P.Gao, M.K.Nazeeruddin, M.Gratzel, S.Ahmad, *Energy Environ. Sci.*,**2015**,8, 2946−2953.

[28] P. Qin, S. Paek , M. I. Dar, N. Pellet , J. Ko, M. Grätzel, M. K. Nazeeruddin, *J. Am. Chem. Soc.*,**2014**,136, 8516−8519.

[29] P. Qin, H. Kast , M. K. Nazeeruddin, S. M. Zakeeruddin, A. Mishra, P. Bäuerle, M. Grätzel, *Energy Environ. Sci*. ,**2014**,7, 2981−2985.

[30] Y.K. Song, S. T.Lv , X.C. Liu, X.G. Li , S.R. Wang, H.Y. Wei, D.M. Li, Y. Xiao, Q.B. Meng, *Chem. Commun.***2014**,50, 15239−15242.

[31] J.J. Wang, S.R. Wang, X.G. Li, L.F. Zhu, Q.B. Meng, Y. Xiao, D. M.Li, *Chem.Commun*. **2014**, 50, 5829−5832.

[32]S.T.Lv, L.Y.Han, J.Y.Xiao, L.F. Zhu, J.J. Shi, H.Y.Wei, Y.Z.Xu, J.Dong, X.Xu, D.M. Li ,S.R. Wang , Y.H. Luo, Q.B. Meng, X.G. Li , *Chem. Commun*.,**2014**, 50, 6931−6934.

[33]L.F.Zhu, J.Y.Xiao, J.J.Shi, J.J.Wang, S.T. Lv, Y.Z.Xu, Y.H.g Luo, Y. Xiao, S.R.Wang, Q.B.Meng, X.G. Li, D.M.Li, *Nano Res.*, **2015**,8, 1116−1127.

[34]Y.K.Wang, Z.C.Yuan, G.Z.Shi, Y.X.Li, Q.Li, F.Hui, B.Q.Sun, Z.Q.Jiang, L.S.Liao, *Adv. Funct. Mater*. **2016**, 26, 1375–1381.

[35]X.C.Liu, L.F.Zhu, F.Zhang, J.You, Y.Xiao, D.M.Li, S.R.Wang, Q.B.Meng, X.G.Li. *Energy Technol.* **2016**, DOI: 10.1002/ente.201600303.

[36]X.Y.Liu, F.Zhang, X.C.Liu, M.N.Sun, S.R.Wang, D.M.Li, Q.B.Meng, X.G.Li, *J.Energy.Chem,***2016**, 25,702-708.

[37]F.Zhang, C.Y.Yi, P.Wei, X.D. Bi, J.S. Luo, G.Jacopin, S.R. Wang, X.G. Li , Y.Xiao , S. M. Zakeeruddin, M. Grätzel , *Adv. Energy Mater*. **2016,** 6, 1600401.

[38] Y.S. Liu, Z.R.Hong, Q.Chen, H.J.Chen, W.H.Chang, Y.Yang, T.B.Song, Y.Yang, *Adv. Mater.* **2016**,28,440.

[39]C.H. Huang, W.F. Fu, C.Z. Li, Z.Q.Zhang, W.M.Qiu, M.M.Shi, P.Heremans, A.Jen, H.Z. Chen, *J. Am. Chem. Soc.*,**2016**, 138,2528.

[40] F.Zhang, X.M. Zhao, C.Y. Yi, D.Q. Bi, X.D. Bi, P. Wei, X.C.Liu, S.R.Wang, X.G.Li, S.M.Zakeeruddin, M. Grätzel, *Dyes and Pigments*, **2016**,DOI: 10.1016/j.dyepig.2016.08.002

[41] S. Karthikeyan, M. Thelakkat, *Inorg. Chim. Acta.*, **2008**,36, 635−655.

[42] I. Neogi, S. Jhulki, M. Rawat, R.S. Anand, T. J. Chow, J. N. Moorthy, *RSC Adv.*,**2015**, 5,26806−26810.

[43]P. Cusumano, S. Gambino, *J. Electron. Mater.* , **2007**,37, 231−239.

[44]D. Poplavskyy ,J. Nelson, *J. Appl. Phys.*, **2002**,93, 341−346.

[45] A. Krishna, D. Sabba, H. Li, J. Yin, P. P. Boix, C. Soci, S. G. Mhaisalkar ,A. C. Grimsdale, *Chem. Sci.*, **2014**,5, 2702−2709.

[46] T. Krishnamoorthy, F. Kunwu, P. P. Boix, H. Li, T. M. Koh,W. L. Leong, S. Powar, A. Grimsdale, M. Gratzel, N. Mathews,S. G. Mhaisalkar, *J. Mater. Chem. A*, **2014**,2, 6305−6309.

[47] J. B. You , Z. R. Hong , Y. Yang , Q. Chen , M. Cai , T. B. Song ,C. C. Chen , S. R. Lu , Y. S. Liu , H. P. Zhou , Y. Yang , *ACS Nano*, **2014**,8, 1674−1680.

[48] C.Y. Yi, X. Li, J.J. Luo, S.M.Zakeeruddin, M.Grätzel, *Adv. Mater*,**2016**, 28,2964.

[49] Y.S. Liu, Q.Chen, H.S. Duan,H.PZhou, Y.Yang, H.J.Chen, S.Luo, T.B.Song, L.Dou, Z.R. Hong ,Y.Yang, *J. Mater. Chem. A*, **2015**,3 , 11940−11947.

[50] L.L. Zheng, Y.H. Chung, Y.Z. Ma, L.P. Zhang, L.X. Xiao,Z.J.Chen, S.F.Wang, B.Qu , Q.H.Gong, *Chem. Commun*, **2014**,50, 11196-11199

[51]D.Gebeyehu, M.Pfeiffer, B.Maennig, J.Drechsel, A.Werner, K.Leo, *Thin Solid Films*,**2004**,451-452 ,29-32.

[52] P. Schillinsky, C. Waldauf, and C. J. Brabec, *Appl. Phys. Lett*. **2002**,81, 3885.

[53] V. D. Mihailetchi, H. Xie, P. W. M. Blom, *Appl. Phys. Lett*. **2002**, 87, 203502.

[54] G. Xing , N. Mathews , S. Sun , S. S. Lim , Y. M. Lam ,M. Grätzel , S. Mhaisalkar , T. C. Sum , *Science*, **2013**,342,344.

[55]F.G.Zhang, X.C.Yang, Ming .Cheng,W.H. Wang ,L.C. Sun, *Nano Energy*, **2016**,20, 108−116.

[56] W. Z. Gao, S. R. Wang, Y. Xiao, X. G. Li, *Dyes. Pigm,***2013***,* 97, 92.

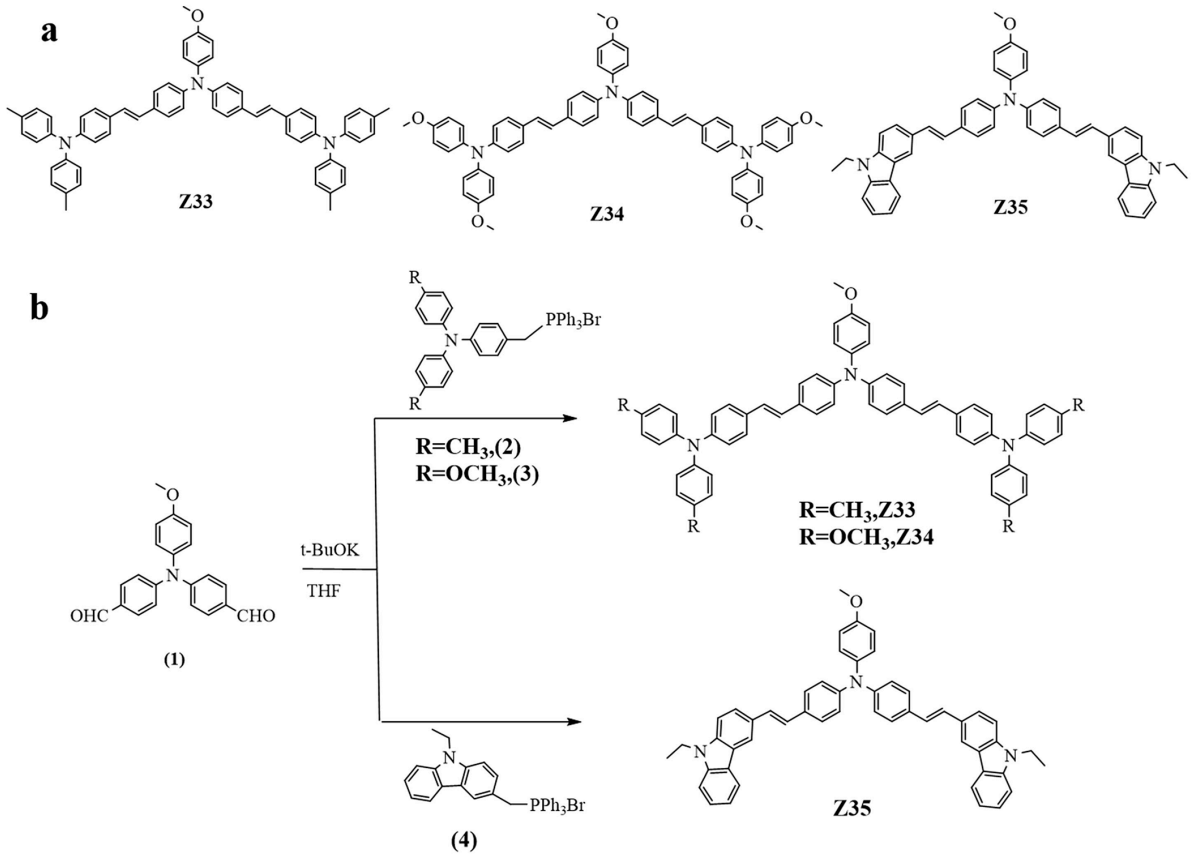

Figure 1 (a) Molecular structures of three HTMs; (b) Synthetic route for three HTMs.

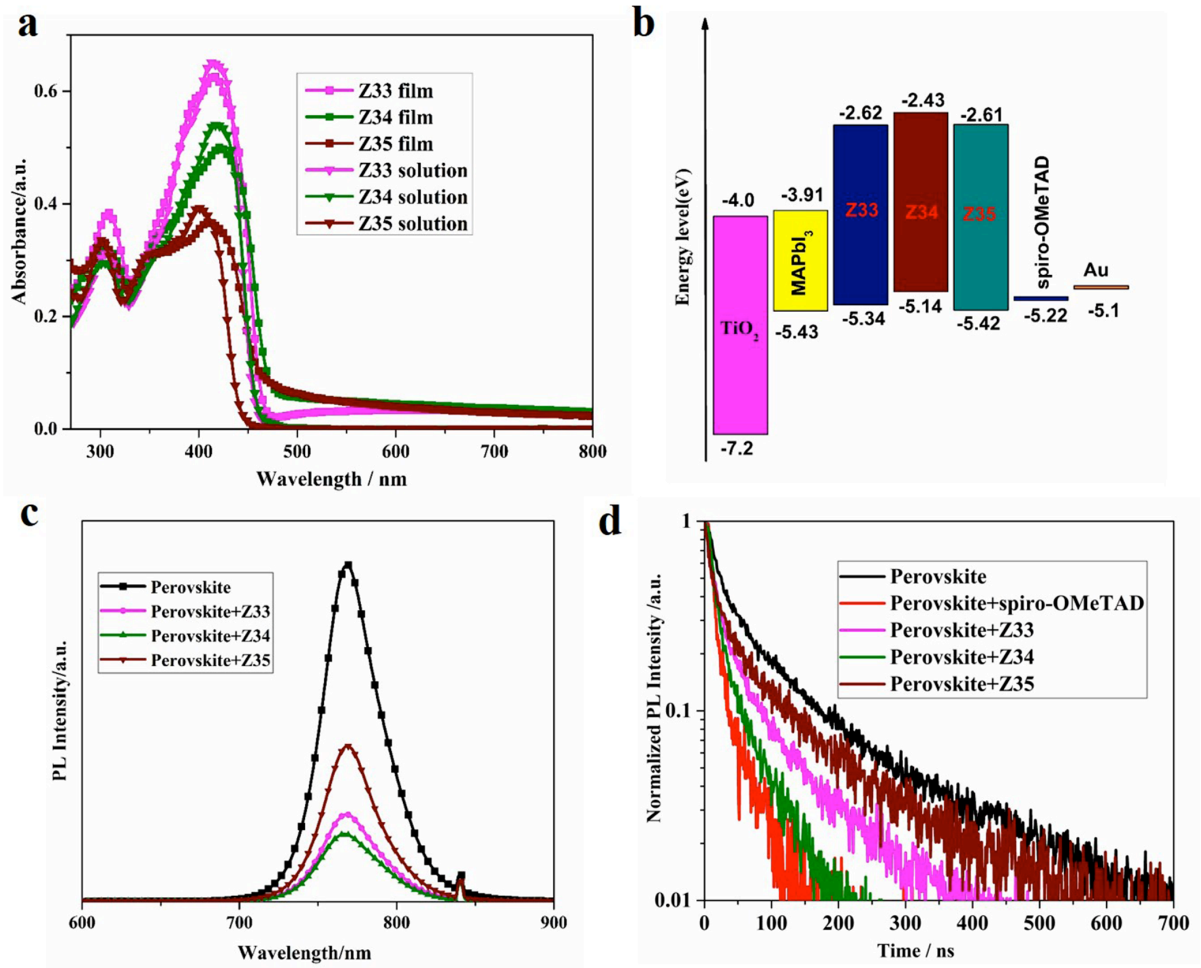

Figure 2 (a) UV-Vis absorption spectra of the HTMs in THF solution(c = 1.0×10^{-5} mol L^{-1}) and on glass ;(b) Energy level diagram of the corresponding materials used in perovskite solar cells;(c) Photoluminescence (PL) spectra for different materials on glass; (d)Normalized time-resolved photoluminescence spectra of corresponding samples.

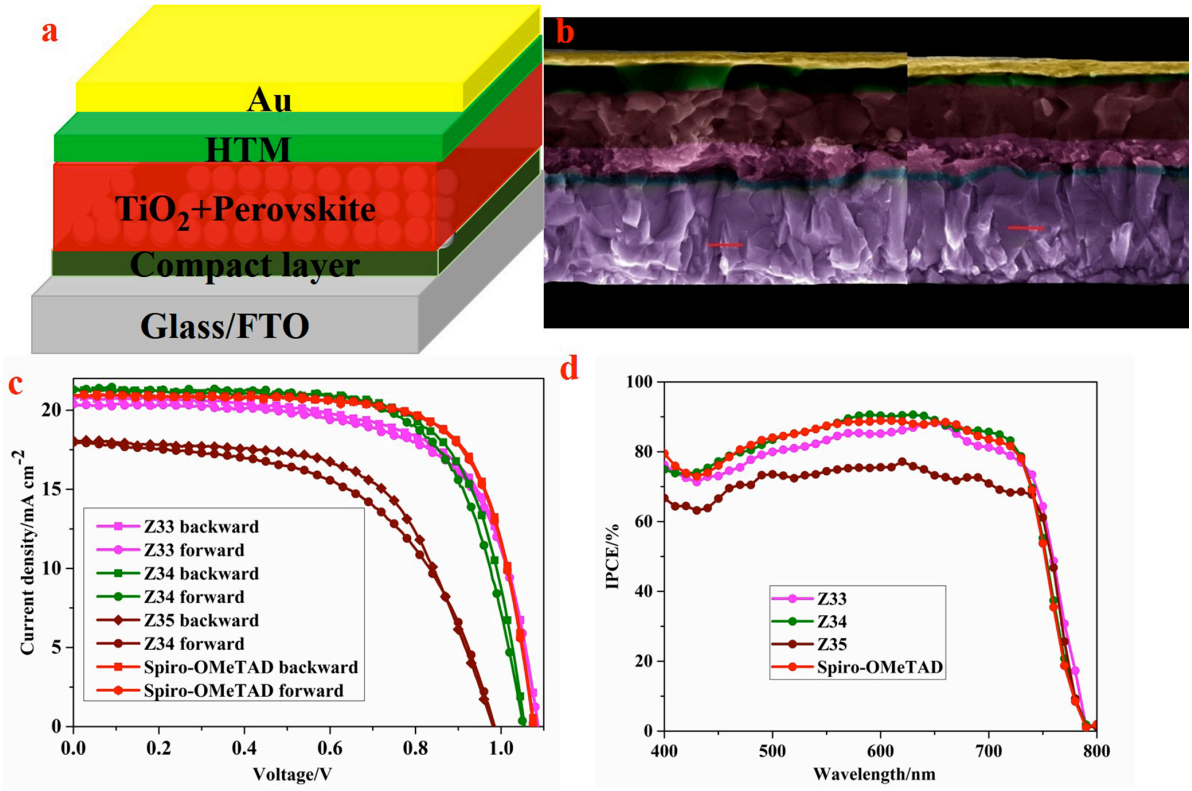

Figure 3 (a) Diagrammatic representation of photovoltaic device structure; (b) Cross-sectional SEM image of the representative device, left (spiro-OMeTAD) and right (Z34), the scale bar is 200 nm;(c) Current-voltage hysteresis curves of perovskite solar cells comprising champion devices with HTMs measured starting with backward scan and continuing with forward scan; (d) IPCE spectra of the devices based on Z33-Z35 without dopants and *spiro*-OMeTAD with additives and dopants.

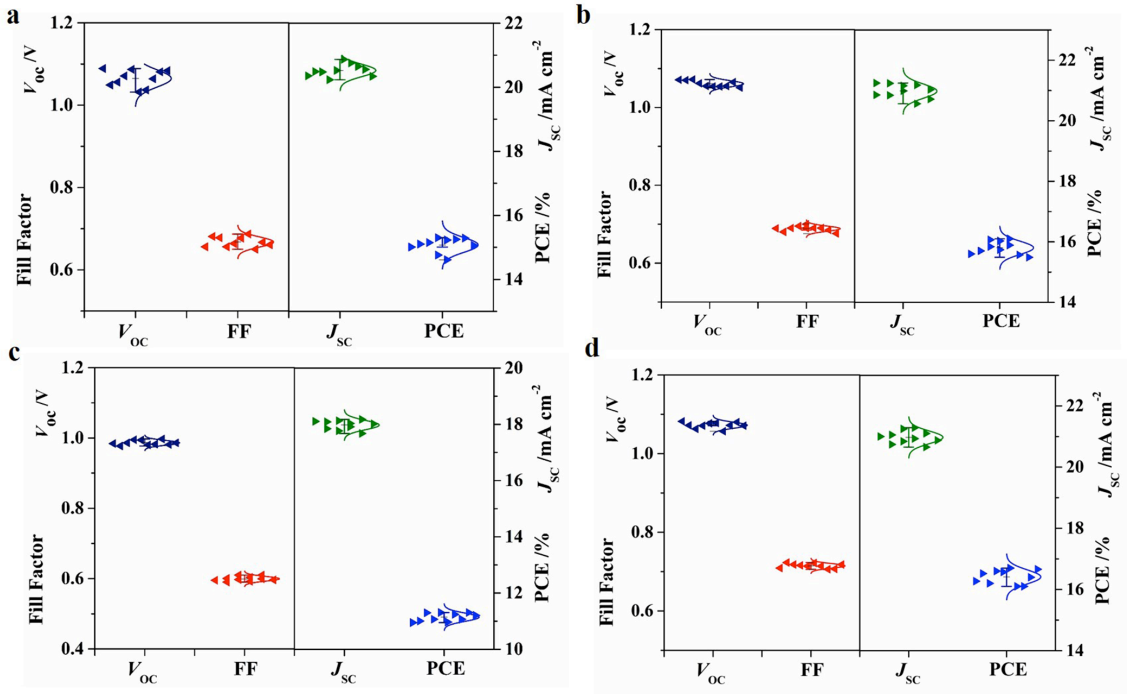

Figure 4 Statistical deviation of photovoltaic parameters for 10 different solar cells using different HTMs: (a) Z33; (b) Z34; (c) Z35;(d) *spiro*-OMeTAD

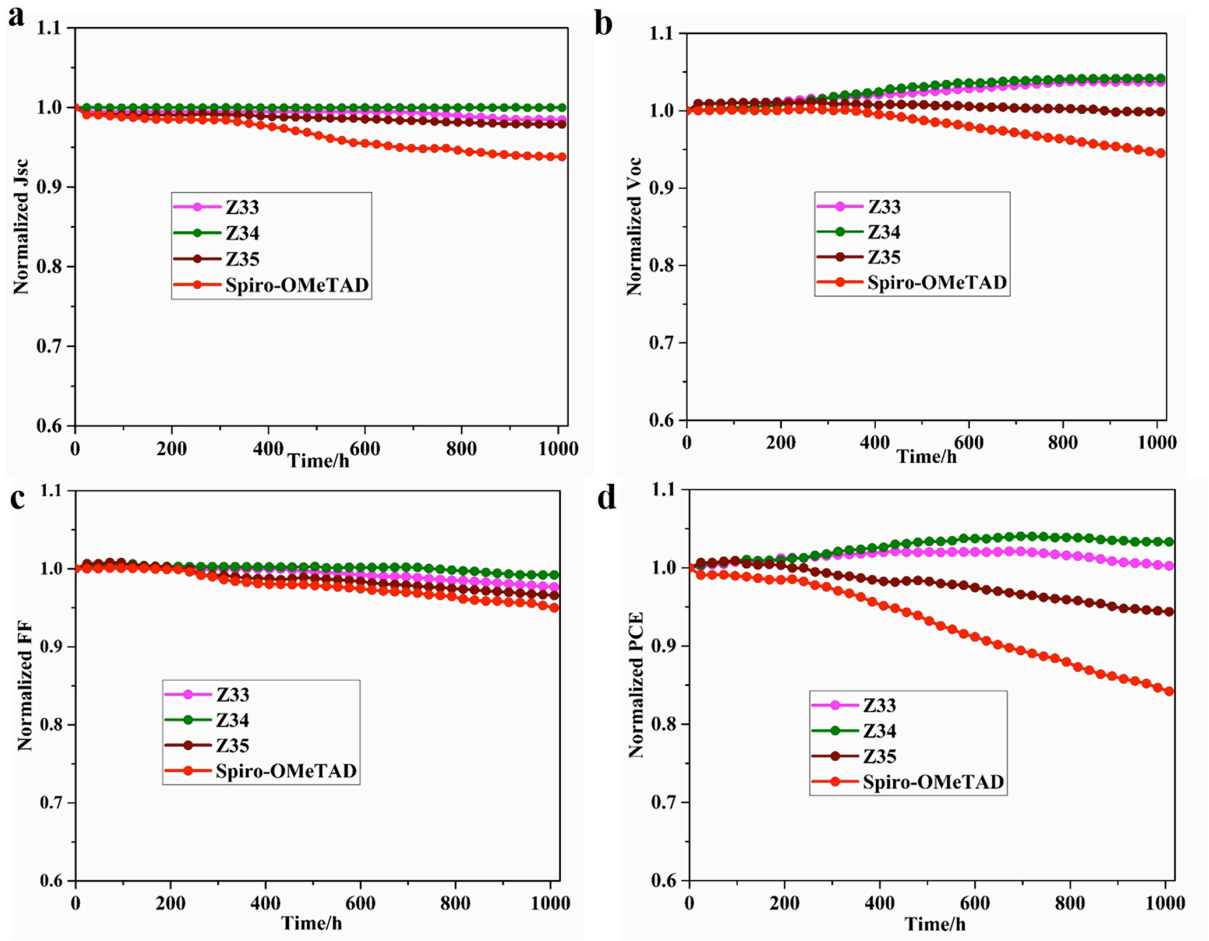

Figure 5 The stability of Z33-Z35 and *spiro*-OMeTAD -based perovskite solar cells in ambient air without encapsulation

Table 1 Photophysical, electrochemical data and thermal characteristics of three HTMs

HTM	$\lambda_{abs/max}$ (nm)	E_g(eV)	HOMO(eV)	LUMO(eV)	T_d(ºC)	T_g(ºC)
Z33	414[a] /416[b]	2.72[c] 3.03[d]	-5.34[c] -4.35[d]	-2.62[c] -1.32[d]	432.3	96.2
Z34	418[a] /422[b]	2.71[c] 3.02[d]	-5.14[c] -4.23[d]	-2.43[c] -1.21[d]	417.2	106.1
Z35	403[a] /414[b]	2.81[c] 3.23[d]	-5.42[c] -4.38[d]	-2.61[c] -1.15[d]	402.2	89.1

[a)]: UV-Vis absorption of THF solution($c = 1.0\times10^{-5}$ mol L^{-1}) ;[b)]: UV-Vis absorption of the films; [c)]: experiment calculation values (HOMO levels is measured by photoemission yield spectroscopy); [d)]:theoretical calculation values.

Table 2 *J-V* curves of HTMs based devices under different scan directions with bias step of 5 mV

HTM		J_{sc}(mA cm^{-2})	V_{oc}(V)	*FF*	PCE (%)
	backward	20.525	1.087	0.66	15.4
Dopant-free Z33	forward	20.386	1.087	0.66	15.2
	avg	**20.456**	**1.087**	**0.66**	**15.3**
	backward	21.245	1.055	0.70	16.1
Dopant-free Z34	forward	21.295	1.051	0.68	15.7
	avg	**21.270**	**1.053**	**0.69**	**15.9**
	backward	18.073	0.981	0.61	11.3
Dopant-free Z35	forward	17.968	0.985	0.55	10.2
	avg	**18.020**	**0.983**	**0.58**	**10.8**
	backward	20.932	1.078	0.72	16.7
spiro-OMeTAD +Li+tBP	forward	20.940	1.076	0.72	16.5
	avg	**20.936**	**1.077**	**0.69**	**16.6**
Z33+Li+tBP		12.978	0.984	0.33	4.4
Z34+Li+tBP		15.100	0.935	0.47	6.7
Z35+Li+tBP		16.369	0.939	0.48	7.7
Dopant-free spiro-OMeTAD		16.692	0.881	0.25	3.9

Three novel dopant-Free D-π-D-π-D conjugated hole transport materials with tunable energy levels are developed for perovskite solar cells exhibiting excellent power conversion efficiency (PCE) of 16.1 % for Z34 which is comparable to the state-of-art doped *spiro*-OMeTAD. Moreover, the device based on the three HTMs are more stable than that of *spiro*-OMeTAD based device in ambient air.

Keyword: hole transport material; dopant-free; perovskite solar cell; low- cost

Fei Zhang, Xicheng Liu, Chenyi Yi, Dongqin Bi, Jingshan Luo , Shirong Wang [*], Xianggao Li[*] , Yin Xiao , Shaik Mohammed Zakeeruddin [*], Michael Grätzel[*]

Novel Dopant-Free D-π-D-π-D Conjugated Hole Transport Materials with Tunable Energy Levels for Efficient and Stable Perovskite Solar Cells

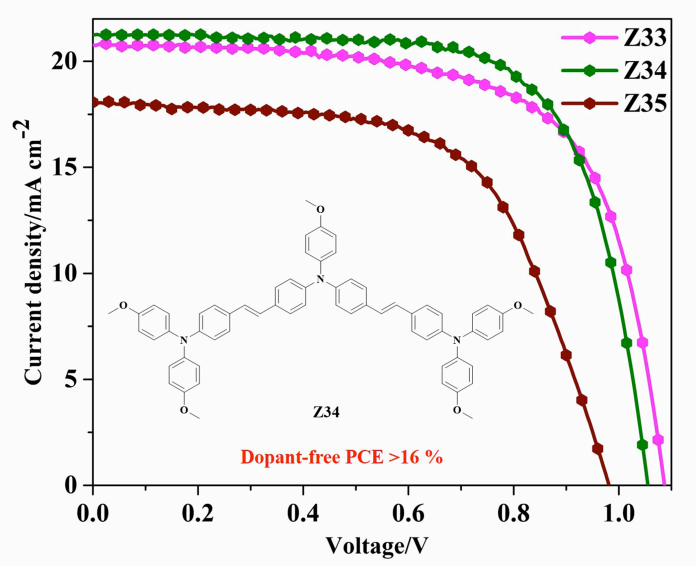

The authors would like to acknowledge the WILEY-VCH Verlag GmbH&Co. KgaA, Weiheim Publishers Limited for accepting to publish in the ChemSusChem.